Published in final edited form as:
Fly (Austin). 2008 ; 2(6): 269–279.

The role of the RING-finger protein Elfless in Drosophila spermatogenesis and apoptosis

Jason C. Caldwell[1], **Mei-ling A. Joiner**[2], **Elena Sivan-Loukianova**[1], and **Daniel F. Eberl**[1,*]

1*Department of Biology, University of Iowa, Iowa City, Iowa USA*

2*Cardiology Division, Department of Internal Medicine, University of Iowa, Iowa City, Iowa USA*

Abstract

elfless (CG15150, FBgn0032660) maps to polytene region 36DE 5′ (left) of *reduced ocelli/Pray for Elves (PFE)* on chromosome 2L and is predicted to encode a 187 amino acid RING finger E3 ubiquitin ligase that is putatively involved in programmed cell death (PCD, e.g., apoptosis). Several experimental approaches were used to characterize CG15150/*elfless* and test whether defects in this gene underlie the male sterile phenotype associated with overlapping chromosomal deficiencies of region 36DE. *elfless* expression is greatly enhanced in the testes and the expression pattern of UAS-*elfless*-EGFP driven by *elfless*-Gal4 is restricted to the tail cyst cell nuclei of the testes. Despite this, *elfless* transgenes failed to rescue the male sterile phenotype in *Df/Df* flies. Furthermore, null alleles of *elfless*, generated either by imprecise excision of an upstream P-element or by FLP-FRT deletion between two flanking piggyBac elements, are fertile. In a gain-of-function setting in the eye, we found that *elfless* genetically interacts with key members of the apoptotic pathway including the initiator caspase Dronc and the ubiquitin conjugating enzyme UbcD1. DIAP1, but not UbcD1, protein levels are increased in heads of flies expressing Elfless-EGFP in the eye, and in testes of flies expressing *elfless*-Gal4 driven Elfless-EGFP. Based on these findings, we speculate that Elfless may regulate tail cyst cell degradation to provide an advantageous, though not essential, function in the testis.

Keywords

Drosophila; RING finger; apoptosis; spermatogenesis; male sterile; pPTGAL; piggyBac; *dronc*; *ubcD1*

Introduction

Spermatogenesis[1-4] is a continuous process that begins at the most immature end of the testis, the gonial region, distal from the seminal vesicle. The stereotypic developmental process of spermatogenesis begins with a single germline cell produced at the gonial tip that travels along the length of the testis, dividing, differentiating and maturing, before ultimately giving rise to fully formed sperm. At the onset of the proliferation phase, occurring at the gonial tip, an unequal cell division from a precursor germline stem cell, tethered to a hub cell, gives rise to a primary spermatogonial cell. In synchrony with the germline stem cell division, two somatic cyst progenitor cells undergo unequal division to form a head cyst cell and a tail cyst cell, which together surround the spermatogonial cell as it undergoes its several divisions. The cyst cells do not divide during the spermatogenesis program. Within the cyst envelope, the primary

*Correspondence to: Daniel F. Eberl; Department of Biology; The University of Iowa; Iowa City, Iowa 52242-1324 USA; Tel.: 319.335.1323; Fax: 319.335.1069; Email: daniel-eberl@uiowa.edu.

spermatogonial cell undergoes four rounds of mitotic division to give rise to 16 spermatogonial cells. Cytokinesis is incomplete during these mitotic divisions, leaving cytoplasmic bridges known as ring canals connecting the cytoplasm of the diploid spermatogonial cells.[5] A specialized cytoskeleton organelle found in the germ line, called the fusome, runs between all of these ring canals and originates from a spectrin-rich structure, called the spectrosome, found in the spermatogonial cells.[6,7] These bridges persist throughout the remaining stages of spermatogenesis[8] and are only degraded later when the mature sperm are individualized.

The 16 germline cells in each cyst then enter a prolonged growth phase with marked increase in transcription levels and increase their cell volume by nearly 25-fold before initiating a meiotic program to give rise to a 64 haploid spermatid cyst. As these haploid cells mature, their mitochondria fuse to form a specialized mitochondrial derivative called a nebenkern. At this stage, the post-meiotic spermatocyst has traveled about two-thirds the length of the testes and, during the cytodifferentiation phase of spermatogenesis, the mature nebenkern begins to elongate with the growing axonemal tail extending from the spermatid. In concert, the two cyst cells undergo distinct morphological changes where the head cyst cell surrounds the spermatid nuclei and the tail cyst cell elongates along with the growing flagellar tail assembly.[2] The tails of the 64 spermatids reach about 2 mm in length while the spermatid DNA condenses and the unit completes cytodifferentiation (Fig. 1).

Sperm individualization is the final stage of spermiogenesis and this process has recently been demonstrated to be dependent on apoptotic machinery.[9-13] Here complexes of actin-rich proteins, the individualization complexes (i.e., the investment cones), travel the length of the spermatids to remove syncytial cytoplasm (Fig. 1B) which eventually collects at the base of the spermatids to form a so-called waste bag; each spermatid is now ensheathed in its own plasma membrane. When each spermatid is fully individualized, the cysts and spermatids coil and the spermatozoa are transferred to the seminal vesicles for storage and, later, fertilization.[14]

Flies trans-heterozygous for polytene region 36DE deficiencies *Df(2L)TW119* and *Df(2L) TW201* (reviewed in ref. [15]) exhibit male sterility, deafness and reduced ocelli (Fig. 2B). The latter two phenotypes are due to disruptions in *btv*/*DHC36D* (FBgn0023096)[16] and *Pray for Elves/rdo* (FBgn0243486),[17] respectively. In *Df(2L) TW119*/*Df(2L)TW201* overlapping deficiency males (henceforth *Df/Df*), the mature sperm are fully formed, yet are amotile (Fig. 2A). The two cyst cells surrounding the mature 64-unit sperm bundle fail to be degraded and the spermatids that constitute this bundle are not individualized (Fig. 2A). Overlapping deficiency males court and mount females, however their initiation and duration of courtship is generally longer and their successful attempted copulation rate is lower due to altered song production and coordination defects caused by *btv*-associated deafness.[18,19] Furthermore, despite the copulation efforts of *Df/Df* males, the sperm are amotile and therefore fail to enter the seminal vesicle, preventing sperm transfer and fertilization.

Previous studies in flies indicate that ultrastuctural or physiological defects associated with disruption of the ciliated neurons of the Drosophila hearing organ are often likewise exhibited in the sperm tails; i.e., deafness and male sterility are intimately linked through dysfunction of common microtubule arrangements.[16,20-23] Indeed, sperm flagella and the ciliated chordotonal sensory neurons in the antenna are composed of the typical 9 × 2 arrangement of microtubule doublets (+0 in chordotonals, +2 in sperm flagella). Courtship, coordination and deafness defects are also apparent in two extant alleles of *beethoven*, btv^{5P1} and btv^{k07109}; however, males are fertile and their sperm are motile, although their successful copulation rate is reduced because of the coordination defects.[24] Based on the evidence that the two extant *btv* alleles and several P-element derived alleles of *DHC36D*[16] only exhibit deafness, it was

likely that the male sterile phenotype associated with deletion of region 36DE was due to disruption of a distinct locus.

Initially, there were several uncharacterized candidates within this large deficiency overlap including several small predicted genes: CG5674 (with exons nested in the introns of *btv*), CG5693, CG15149, CG31740 and CG15150 (Fig. 2C). CG15150, which we here name *elfless*, (Fig. 2C and D) was further investigated as this gene had been previously isolated from testis cDNA pools[25] and was therefore considered a promising candidate for the fertility defects seen in *Df/Df* flies. In this paper we describe experiments showing that *elfless* encodes a RING-finger protein, is expressed specifically in the tail cyst cells, but does not account for the male sterility in this interval. Mis-expressing *elfless* in most tissues is lethal, but we examine its possible biological role by mis-expressing it in the eye, a tissue dispensable for viability.

Results

elfless encodes a predicted nuclear RING-finger protein

FlyBase[33] predicts the genomic region of *elfless* to be 1300 basepairs, comprising a 15 basepair 5′UTR, a 587 basepair 3′UTR, 3 exons and 2 short introns (Fig. 2D). The full-length cDNA of *elfless* is 564 basepairs. The Berkeley Drosophila Genome Project (BDGP) isolated thousands of cDNA clones in large-scale screens of libraries from different Drosophila tissues. One such clone, AT24563 (a cDNA from a Drosophila Adult Testes Library), contains a 1,194 basepair full-length *elfless* cDNA, with 3′ and 5′ UTR ends (Fig. 3); this cDNA clone was used for further analyses, as discussed below.

elfless is predicted to encode a 187 amino acid zinc finger Cys3-His-Cys4 RING protein[33] (C3HC4 RING; Fig. 2E); amino acids 135–174 align with the reported RING consensus sequence[34] [C-$X_{(2)}$-C-$X_{(9-39)}$-C-$X_{(1-3)}$-H-$X_{(2-3)}$-C-$X_{(2)}$-C-$X_{(4-48)}$-C-$X_{(2)}$-C] (where X is any amino acid, C is Cys and H is His; Fig. 3). RING domains are involved in protein-protein interactions, including binding to E2 ubiquitin conjugating enzymes and have recently been shown to function as E3 ubiquitin ligases and essential regulators of apoptosis.[35-37] Indeed, the RING finger protein Elfless is predicted to encode an E3 ubiquitin ligase.[33] Furthermore, in a yeast two-hybrid assay, Elfless was shown to interact with the E2 ubiquitin conjugating enzyme UbcD1 (FlyGrid; http://biodata.mshri.on.ca/fly_grid/).

BLASTp analysis with the Elfless protein sequence revealed no strong matches (>50% identity), but, in general, it was found that Elfless shares some similarity with C3HC4-type RING-finger proteins in *D. melanogaster* and other organisms, almost exclusively in the RING domain. Similarly, PSORT (http://psort.hgc.jp) analysis also identified a C3HC4 RING domain. Additionally, PSORT identified a sequence (PPNKRIK; Fig. 3) with 65.2% probability to be a nuclear localization signal.

elfless is expressed in the tail cyst cells in testes

Based on the EST data we wanted to determine the *elfless* expression pattern. Initially, our focus was primarily on adult tissues for two reasons: (1) we were investigating *elfless* as a candidate for male sterility and (2) data collected from the BDGP in situ screen indicated that *elfless* has no detectable embryonic expression pattern. Real time PCR analysis indicates that *elfless* expression is strongly enhanced in the testes and whole males, while it is virtually undetectable in males with testes removed (carcasses) and whole females (Fig. 4; see Fig. for complete statistical analysis).

To understand more completely the spatial and temporal expression of elfless, we employed the pPTGAL vector[32] to generate *elfless*-Gal4. In this construct, *elfless* regulatory sequences were cloned upstream of Gal4 and therefore Gal4 expression follows an *elfless*-specific pattern.

A 2.27 kilobase fragment that includes the *elfless* TATA box and presumptive 5′ regulatory elements was cloned into pPTGAL, and transgenic flies with the resulting plasmid were used as *elfless*-Gal4.

In testes, *elfless*-Gal4 driven GFP expression was prominent in the cytoplasm of cells whose position and morphology are consistent with tail cyst cells (Fig. 5D–F). Outside of testes, no reproducible GFP expression was detected. Expression was assayed in all embryonic stages, in L1 and L3 larvae, in early- and mid-pupal stages and in adults (data not shown). Sporadic GFP expression was seen in a very small number of cells in the L3 salivary glands and Malpighian tubules—the position of these cells was not reproducible, suggesting that this expression represents noise in the Gal4 system rather than real *elfless* expression.

To determine the subcellular localization of Elfless, a UAS construct containing *elfless* cDNA C-terminally fused with EGFP (UAS-*elfless*-EGFP) was generated. *elfless*-EGFP expression driven by *elfless*-Gal4 is restricted to a subset of nuclei whose location is again consistent with the tail cyst cell nuclei. Expression is apparent neither in the 64-unit sperm bundle nuclei nor in the head cyst cell nuclei that are proximal to the spermatid nuclei (Fig. 5A). Nuclear localization is consistent with the PSORT prediction of a nuclear localization signal. To confirm nuclear localization, a genetic approach to counter-staining nuclei was undertaken with the reporter construct, UAS-RedStinger-nls, that expresses a nuclear localized RFP (nuc*Ds*Red), cloned from the coral *Discosoma*.[29] In *w*; UAS-RedStinger-nls/+; UAS-*elfless*-EGFP/*elfless*-Gal4 testes, *elfless-EGFP* expression co-localizes with nuc*Ds*Red, confirming that Elfless-EGFP is indeed a nuclear localized fusion protein (Fig. 5B and C). When testes from the parental UAS-RedStinger-nls flies are observed in the absence of a Gal4 driver, significant, spurious expression of nuc*Ds*Red in the spermatid bundle and head and tail cyst cell nuclei is evident (data not shown); this accounts for the incomplete co-localization in Figure 5C. Since GFP alone localizes to the cytoplasm (Fig. 5D–F), the nuclear localization of Elfless-EGFP most likely relies on the predicted nuclear localization signal in the Elfless protein; formal confirmation would require mutating this predicted signal.

To confirm the identity of expressing cells as tail cyst cells, we introduced the tail cyst cell lacZ enhancer trap, *P{lacW}498* (reviewed in ref. [2]), into the *elfless*-Gal4, UAS-*elfless*-EGFP genotype. X-gal staining coincides to a large extent with *elfless*-EGFP expression (Fig. 6). In these flies we found the number of X-gal positive cells to vary considerably from fly to fly; Figure 6 is an example with a larger fraction of the tail cyst cells, but not all of them, labelled (reviewed in ref. [2]).

elfless fails to rescue male sterility in *Df/Df*

Because of the specific *elfless* expression in testes, we wanted to test whether *elfless* is responsible for the male sterility in *Df/Df* males. To this end, a UAS rescue construct, UAS-*elfless*, and a genomic rescue construct, Casper-*elfless*, were generated. The genomic *elfless* construct contains the entire *elfless* coding region and the presumptive upstream regulatory elements (discussed above). Two independent genomic construct insertions, one each on chromosomes 2 and 3, failed to rescue male sterility when *Df/Df* males were crossed to w^{1118} virgin females (N = 10; no offspring produced). In testis squashes, the sperm were amotile and remained encysted like those of the *Df/Df* testes shown in Figure 2A (data not shown).

UAS-*elfless* was generated for expression with the Gal4/UAS system.[31] The UAS-*elfless* construct was generated from the full-length *elfless* cDNA, AT24563, by subcloning into the pUAST vector.[31] As with the genomic *elfless*, UAS-*elfless* driven by *elfless*-Gal4 fails to rescue male sterility in *Df/Df* (N = 10; no offspring produced). In testis squashes the sperm were amotile and remained encysted like those of *Df/Df* (data not shown).

elfless null alleles do not disrupt fertility

To rule out the possibility that failure of *elfless* transgenes to rescue male sterility in a *Df/Df* background was due to a problem with the transgenes, or the alternative possibility that *Df/Df* uncovered more than one fertility locus, we wanted to examine *elfless*-specific loss of function. Therefore, *elfless* null alleles were generated using two genetic techniques: P-element excision and piggyBac-mediated FLP-FRT deletion. The P-element, KG02815,[38] inserted just downstream of the 5′UTR of *PFE* (*rdo*$^{+}$) and 3′ of *elfless* (Fig. 2C), was used in a P-element mobilization screen for imprecise excisions that disrupt *elfless*. 146 total putative excision lines were PCR screened and in two lines, *elfless*$^{KG02815.8b}$ and *elfless*$^{KG02815.15a}$, the entire *elfless* presumptive upstream regulatory region and coding region were deleted while the neighboring predicted genes, CG31740, CG15149 and CG5693, remained intact. These lines are also *rdo*$^{-}$ likely due to a flanking deletion into *PFE;* the exact breakpoints of these deletions were not determined. At the same time as the P-element mobilization screen, the more precise heat shock FLP-FRT technique for generating deletions through recombination between nearby transposon insertions was also performed.[30,39] Two piggyBac insertions, WHf06603 (*rdo*$^{+}$) and WHf06680 (*rdo*$^{-}$), are inserted on either side of *elfless* (Fig. 2C) and FLP-mediated recombination was used to delete the intervening region that includes *elfless,* CG31740, CG15149 and CG5693. Heat shock and crosses were performed as described[30] and two deficiency strains *Df(2L)JCC.YA2* and *Df(2L)JCC.PE2* were isolated.

We wanted to determine if deletion *elfless* blocked or reduced fertility. Fertility of P-element derived deletion lines, *elfless*$^{KG02815.8b}$ and *elfless*$^{KG02815.15a}$ was not significantly reduced compared to wild type controls, and FLP-FRT-derived deletion lines, *Df(2L)JCC.YA2* and *Df(2L)JCC.PE2* showed modest, but significantly reduced fertility that was later determined to be due to the reduced fecundity of the original WHf06680 piggyBac strain (data not shown). Altogether, these data indicate that *elfless* is not essential for fertility. Furthermore, since the FLP-mediated deletions also remove three additional predicted genes, these four genes neither solely nor together are responsible for the male sterility in *Df/Df.*

A gain-of-function role for *elfless* in apoptosis

Since many developmentally restricted genes have no phenotype when expressed ubiquitously, we were surprised to find that UAS-*elfless* mis-expression is embryonic or first instar larval lethal with most Gal4 drivers including: (1) a ubiquitous Gal4 driver *spaghetti-squash*-Gal4 (reviewed in ref. [40]), (2) nervous system drivers *elav*-Gal4 (FBst0008760)[41] and NP6215-Gal4 (FBst0304010),[42] and (3) salivary gland driver *sgs3*-Gal4 (FBst0006870).[43] In contrast, a photoreceptor driver *GMR*-Gal4 (FBal0052387)[44] and the cyst cell driver *elfless*-Gal4 that we describe here, both allow adult survival. Expression with *GMR*-Gal4 resulted in eye defects, as described below. This, together with the lethality associated with mis-expression of *elfless* in other tissues, shows that this molecule is detrimental in many tissues. This conclusion introduced the possibility that this molecule might inappropriately regulate the apoptosis pathway in these various tissues, as other E3 ubiquitin ligases can induce or inhibit apoptosis.[13,35,37,45]

To determine whether ectopic *elfless* could be interfering with the apoptosis pathway, we further explored the gain-of-function eye phenotype with *GMR*-Gal4. We found that *w*; *GMR*-Gal4; UAS-*elfless* flies exhibit morphological defects including missing or extra inter-ommatidial bristles, rather than the stereotypical single inter-ommatidial bristle seen in wild type eyes (Fig. 7A). Furthermore, the eye itself is prone to deformation (Fig. 7B), due to a presumptive loss of ommatidial ultrastructural integrity, and the individual ommatidia also exhibit pigment loss in random patterns over the surface of the eye (Fig. 7A)—pigment loss and structural defects become more advanced as the fly ages (data not shown). Notably, the

size of the eye, despite the roughness and pigment loss, is largely unchanged in this gain-of-function line (Fig. 7A and B).

The ommatidial bristle loss and gain and the pigment loss phenotypes are similar to those exhibited by several members of the apoptosis pathway including *w*; *GMR*-Gal4; UAS-*Dronc*.[46] In this strain, like in *w*; *GMR*-Gal4; UAS-*elfless*, the size of the eye is largely unaffected whereas in other apoptosis pathway lines, like *GMR-hid* and *GMR-rpr* (where *hid* or *rpr* are expressed by direct GMR promoter fusion), the size of the eye is greatly reduced.[47-49] These observations suggested that *elfless* is not a pro-apoptotic gene like *rpr* or *hid*, but may be acting further downstream in the apoptosis pathway.

A key regulator of apoptosis is DIAP1, the Drosophila Inhibitor of Apoptosis 1.[27,37,46,50-53] DIAP1 directly inhibits downstream caspases, Dronc[46,54,55] and Drice[56,57] and prevents cell death. The regulation of Dronc is accomplished through ubiquitination of Dronc via the C-terminal RING domain of DIAP1 in a UbcD1-dependent manner.[37] Contrarily, when the cell receives an intrinsic or extrinsic signal to die, the N-Terminal RHG domains of proapoptotic factors Rpr, Hid and Grim bind to the C-terminal BIR (baculovirus IAP repeat) domain of DIAP1,[58] and thereby antagonize DIAP1/UbcD1-mediated inhibition on the zymogen form of the caspase Dronc. Furthermore, binding of Grim, Rpr and Hid to DIAP1 promotes auto-ubiquitination of DIAP1, again in a UbcD1-dependent fashion.[27,51-53,59] This second level of downregulation of DIAP1 ensures liberation of the initiator caspase, Dronc, which is then able to associate with the adaptor molecule, Dark,[60] and this active complex then processes and activates downstream effector caspases, Drice and Dcp-1,[46,61] that initiate PCD.

Elfless has been experimentally demonstrated to interact with UbcD1 by yeast two-hybrid and, as mentioned above, UbcD1 has been implicated as a key regulator of the apoptosis pathway at the intersection between DIAP1 and the caspases. When *w*; *GMR*-Gal4; UAS-*elfless* was crossed into a *ubcD1* heterozygous mutant background, the eye phenotype became significantly more severe, indicating increased apoptosis, and the vast majority of these flies die as pharate adults (Fig. 7C and D). Conversely, reducing the level of the downstream caspase, Dronc, suppressed the eye phenotype, as the eyes of *w*; *GMR*-Gal4; UAS-*elfless* flies in a *Dronc* heterozygous mutant background show improvement in both the extent of pigmentation loss and overall eye morphology/deformation (Fig. 7E and F). Together these data show that *elfless* genetically interacts with key members of the apoptosis pathway that are downstream of the pro-apoptotic genes (Fig. 9).

To determine whether protein levels of DIAP1 or UbcD1 are affected upon Elfless-EGFP mis-expression in the eye, or overexpression in the tail cyst cells, we isolated protein from heads or testes of flies carrying the appropriate Gal4 driver, with or without the UAS-*elfless*-EGFP construct, and probed Western blots with either DIAP1 or UbcD1 antibodies. We found that in both tissues, DIAP1 protein levels were increased, while UbcD1 protein levels remained unchanged (Fig. 8). These results, together with the genetic interactions, indicate that the apoptosis pathway is affected by these genetic manipulations.

Discussion

Emerging data are now elucidating the roles of key members of the apoptosome, including the caspases Dronc and Drice, in spermatid individualization in Drosophila.[9,13] The molecules are thought to be inhibited by dBruce, a ubiquitin-conjugating enzyme with a BIR domain.[9,10] In effect, dBruce may be acting in the spermatid cysts in a manner similar to another documented BIR-domain protein, DIAP1. In this study, we examined the role of the E3

ubiquitin ligase, Elfless, and show that, consistent with its prediction as a RING finger protein, Elfless interacts with key members of the apoptotic pathway.

Based on our results and the following published observations we propose that Elfless acts to directly or indirectly regulate UbcD1 activity in the apoptotic pathway (Fig. 9). *w*; *GMR*-Gal4; UAS-*elfless* in an otherwise wild type background produces pigment cell defects reminiscent of those of *w*; *GMR*-Gal4; UAS-*Dronc* (Fig. 7A and B). As previously shown, *w*; *GMR*-Gal4; UAS-*Dronc* in a *ubcD1* heterozygous mutant background produces an eye phenotype slightly worse than *w*; *GMR*-Gal4; UAS-*Dronc* alone[37] which suggests that Dronc may also be a target of UbcD1. Finally, inhibition of apoptosis through Dronc is effectively lost in *w*; *GMR*-Gal4; UAS-*Dronc* in a *diap1*/+ background; the eye defects exhibited in these lines are severe and flies die as pharate adults.[55] *w*; *GMR*-Gal4; UAS-*elfless* flies in a *ubcD1*/+ mutant background similarly die as pharate adults (sublethal in males and females; analyzed by χ^2: $p < 0.05$, N = 25 vials/allele; data not shown) and the eye phenotype is significantly worse than that of *w*; *GMR*-Gal4; UAS-*elfless* alone (Fig. 7C and D); pigmentation is absent in these flies and the size of the eye is reduced due to decreased UbcD1-mediated inhibition of Dronc and DIAP1. These data suggested that Elfless may be regulating UbcD1 activity.

While Elfless and UbcD1 had been shown to interact by yeast-two hybrid, we have not been able to confirm a direct association between Elfless and either DIAP1 or UbcD1 by co-immunoprecipitation experiments (data not shown). Nevertheless, it is clear from Western blot analysis that mis-expression of Elfless-EGFP in the eye or testes does not significantly change the level of UbcD1 protein but does increase DIAP1 protein levels (Fig. 8). Thus, if Elfless is downregulating UbcD1 activity, it seems to be doing so without changing UbcD1 levels. Since DIAP1 auto-ubiquitination is UbcD1-dependent, Elfless-mediated downregulation of UbcD1 activity is consistent with reduced DIAP1 auto-ubiquitination and degradation, resulting in higher DIAP1. While on the one hand this would increase the anti-apoptotic activity of DIAP1, UbcD1 downregulation on the other hand would also increase the pro-apoptotic activity of Dronc, effectively circumventing DIAP1, and producing the somewhat mild eye phenotype evident in *w*; *GMR*-Gal4; UAS-*elfless* in an otherwise wild type background. Consistent with this model, in *ubcD1* heterozygotes the eye phenotype is severely worsened and lethality is evident, while in *Dronc* heterozygotes, the eye phenotype is improved.

Although we clearly demonstrate a genetic interaction of *elfless* with *Dronc* and *ubcD1* in PCD and we propose that mis-expressed Elfless in the eye negatively regulates UbcD1 activity, we were unable to ascribe an essential role in fertility to this locus, despite the promising role of this molecule in sperm development based on expression profiling and the *Df*/*Df* male sterility phenotype. Furthermore, an *elfless* transgene is not sufficient to rescue the male sterility associated with these deficiencies in polytene region 36DE. Despite the lack of a sterility phenotype when the RING finger protein encoded by *elfless* is deleted from the genome, the fact that *elfless* is functionally retained in the genome by selection indicates that *elfless* performs an important and advantageous, albeit redundant, function in the testes. Thus, while in laboratory vials, males are able to produce normal numbers of offspring, subtle functional differences can be quite significant in wild populations. What advantage could Elfess provide in the tail cyst cell? One possibility is that mobilization of Elfless in the nuclei of these cells facilitates tail cyst cell degeneration for more efficient resorption; sperm release from the cyst can still take place, but there may be a physiological burden on the testis during the life-time of the fly. The fact that Elfless is in the nucleus may suggest that it targets gene expression at this transitional stage of tail cyst cells. Full activation of apoptosis by Elfless in tail cyst cells is unlikely, as Elfless is nuclear, and no TUNEL staining in wildtype testes appears in the late stage cysts (data not shown). Nevertheless, apoptosis signaling can be quite different in varying developmental contexts (reviewed in refs. [10] and [13]), and there is precedent for enlisting branches of the apoptotic pathway in different developmental processes. For example,

Caspase-3 is activated in the cystic bulge of the developing spermatocyst,[9] while the correct balance of DIAP1 levels is important for cellular mobilization of border cells and other cells during oogenesis.[62,63] More incisive future approaches will be needed to discern the roles that Elfless and other subtle modulators play in mating and evolution.

Materials and Methods

Animals

Control strains used for fertility tests were of the genotypes w^{1118} (Exelixis isogenic, henceforth *isow*; FBst0006326) and *y w. Df(2L)TW119, cn bw/CyO* (FBab0001642) and *Df(2L) TW201, b/CyO* (FBab0001650)[15] lines were used for deficiency mapping. We will refer to flies carrying these two overlapping deficiencies as *Df/Df*. Genetic interaction studies were performed with the following stocks: *w;; Dronc*^{I24} FRT80/*TM3, Sb* (reviewed in ref. [26]), *Sco/Cyo; GMR-rpr* (reviewed in ref. [27]), w^{1118}; *ubcD1*^{XS347}/*TM3, Sb GMR-sina* (reviewed in ref. [28]) and w^{1118}; *ubcD1*^{598}/*TM3, Sb GMR-sina* (reviewed in ref. [27]). Co-localization with UAS-*elfless*-EGFP was analyzed with w^{1118}; P{UAS-RedStinger}4/*CyO* (FBst0008546)[29] and with the *y w; P{lacW, w*$^{+}$*}498* tail cyst cell enhancer trap line.[2] See references in text for genotypes of Gal4 drivers used in these analyses. Transposable element strains are described below.

Fertility assays

Single newly emerged males were isolated and were allowed to mate with five *isow* or *y w* virgin females, as appropriate, for 2 days. Prior to crossing, isolated males and females were stored separately for 1 day to allow cuticles to sufficiently harden. After 2 days of mating, females were then moved into separate vials and the original vial was likewise retained. Male fertility for each genotype was scored as the average of the total number of offspring that emerged from all vials in a 5-day period (N = 10 males for all genotypes tested).

P-element excisions and piggyBac deletions

The *y*^{1} w^{67c23}*; P{SUPor-P}KG02815* (FBst0012989) P-element was mobilized by crossing to transgenic flies carrying a source of P-transposase, *wg*$^{Sp-1}$*/CyO; ry*^{506} *Sb*^{1} *P{Δ2-3}99B/TM6,Ubx*^{P15} (FBst0002535). y^{-} w^{-} derivatives were screened and independent lines established. Heat shocking larvae for generating FLP-FRT deletions with Exelixis piggyBac insertion lines *isow;* Pbac{WH}f06603 (FBst1020693) and *isow*; Pbac{WH}f06680 (FBst1020745) was performed as described.[30] Likewise, putative deletion lines were isolated and stable stocks generated as described using the Exelixis isogenized *w* strains, P{hsFLP}[1], w^{1118}; *Adv*^{1}*/CyO* (FBst0000006) and w^{1118}; P{hs-hid}2, *wg*$^{Sp-1}$*/CyO* (FBst0007757). Primers used to screen for P-element and piggyBac deletions in the full-length coding regions of *elfless* and the neighboring predicted genes are as follows (Table 1): elfless-FullF and elfless-FullR, CG31740Fwd and CG31740Rev, CG15149Fwd and CG15149Rev and CG5693Fwd and CG5693Rev and the PCR program [{95°C/30 s, 55.9°C/30 s, 72°C/1 min} × 30; {72°C/5 min} × 1].

Cloning

The UAS-*elfless* construct was generated by subcloning the full length *elfless* cDNA from the AT24563 EST clone (Accession #AY113298) into pUAST;[31] this UAS construct was injected into w^{1118} embryos using standard techniques. UAS-*elfless*-EGFP was generated by amplifying the *elfless* cDNA from the AT24563 vector template with primers elf-GWF and elf-GWRv2 (Table 1) and the PCR program [{95°C/30 s, 55.0°C/30 s, 72°C/30 s} × 30; {72°C/5 min} × 1]. The elf-GWF primer has an engineered CACC sequence before the ATG start, to ensure directional cloning into the pENTr entry of the Drosophila Gateway vector system (Invitrogen). The amplified *elfless* cDNA was cloned in the pENTr/D-TOPO vector, sequenced

to verify and subcloned into the Drosophila Gateway pTWG destination vector by the LR recombination reaction as described (Invitrogen and Murphy Lab http://www.ciwemb.edu/labs/murphy/Gateway vectors.html). The final construct was injected at the Model System Genomics Facility at Duke University (http://www.biology.duke.edu/model-system/).

The full-length genomic region of *elfless* was PCR-cloned from Canton S DNA (4040 basepairs into TOPO-XL) with the primers SKF-5′F and SKF-5′R (Table 1) and the PCR program [{95°C/30 s, 54.0°C/30 s, 72°C/5 min} × 30; {72°C/10 min} × 1] and sequenced to verify clone accuracy against the published sequence. This 4040-basepair clone was used to generate an *elfless* genomic rescue clone by restriction enzyme digest subcloning into pCaSpeR4. To generate an *elfless*-Gal4 driver, a 2.27 kilobase fragment that includes the *elfless* TATA box and presumptive regulatory elements was subcloned from the genomic clone in TOPO-XL into the pPTGAL vector.[32] Both resulting plasmids were injected by the Model System Genomics Facility at Duke University.

Real time PCR

Total RNA was isolated from tissues indicated in text using the RNeasy mini kit (Qiagen) with DNaseI treatment (Qiagen) per kit instructions. For real time PCR, first strand synthesis was performed on isolated total RNA using the Superscript III First Strand Synthesis System for RT-PCR (Invitrogen) and oligo$(dT)_{20}$ primer per kit instructions. Real time PCR was carried out with isolated cDNAs and the SYBR Green PCR Master Mix (Applied Biosystems) with *Gapdh2* control primers Gapdh2-f and Gapdh2-r and *elfless* primers elfless-realtimeF and elfless-realtimeR (Table 1). To control for pipetting errors, cDNAs from a biological sample were amplified in triplicate for both control and *elfless* primers; three biological samples per strain per genotype were analyzed. Real time PCR was performed using the following cycling conditions: [{95°C/10 min} × 1; {95°C/15 s, 60°C/1 min} × 40] and a single dissociation protocol {60°C + 35°C/20 min}. In the dissociation step, a single peak was obtained for *Gapdh2* and *elfless* primers indicating only a single, specific product was amplified.

Scanning electron microscopy

Heads were isolated and fixed in 2.5% glutaraldehyde for 24 hours at 4°C, postfixed in 1% OsO_4/Phosphate Buffer for 1 hour, dehydrated in an ethanol series, critical-point dried and finally sputter coated with a layer of Gold/Palladium. Images were taken on a Hitachi S-4000.

Western analysis

Fifty pairs of testes or 20 heads from control and Elfless-EGFP-expressing animals were homogenized in buffer (150 mM NaCl, 0.05% Nonidet p40, 50 mM Tris-HCl, pH 8.0 and protease inhibitors (Roche)). After 3 h of incubation at 4°C followed by 15 min centrifugation at 4000 g, crude extract was twofold diluted with lysis buffer (50 mm Tris/HCl, pH 8.0, 150 mm NaCl, 0.05% NP40, 5 mm EDTA, 0.2% BSA, 0.02% NaN_3 and protease inhibitors). Lysate (20 μg/lane) from each preparation was run out on a 4–12% polyacrylamide gel. Blots were probed with antibodies against DIAP1 (gift of Hermann Steller), UbcD1 (gift of Hyung Don Ryoo) and Hsp60 (Sigma).

Statistical analysis

All data were analyzed using SAS version 6.12 (Sas Institute Inc., Cary, NC, USA). Real time PCR and fertility data were analyzed by ANOVA with pair-wise Tukey and counts for the *w*; *GMR*-Gal4; UAS-*elfless* with *ubcD1* and *Dronc* alleles were analyzed by χ-square with an expected 1:1:1 Mendelian ratio.

Acknowledgements

We would like to thank Grace Boekhoff-Falk for critical reading of the manuscript. Steve DiNardo, Andreas Bergmann, Yehuda Ben-Shahar, Toshi Kitamoto, Wayne Johnson, Barbara Sisson and the Bloomington Drosophila stock center for providing fly stocks, the Duke University Model Systems Genomics Facility for injection of the *elfless* constructs, and the University of Iowa Central Microscopy Facility for SEM use. This work was supported by NIH grant DC04848 to Daniel F. Eberl.

Abbreviations

RING, really interesting new gene; GMR, *glass* multimer reporter; PCD, programmed cell death.

References

1. Castrillon DH, Gönczy P, Alexander S, Rawson R, Eberhart CG, Viswanathan S, DiNardo S, Wasserman SA. Toward a molecular genetic analysis of spermatogenesis in *Drosophila melanogaster*: characterization of male-sterile mutants generated by single P element mutagenesis. Genetics 1993;135:489–505. [PubMed: 8244010]
2. Gönczy P, Viswanathan S, DiNardo S. Probing spermatogenesis in Drosophila with P-element enhancer detectors. Development 1992;114:89–98. [PubMed: 1576968]
3. Gönczy P, DiNardo S. The germ line regulates somatic cyst cell proliferation and fate during Drosophila spermatogenesis. Development 1996;122:2437–47. [PubMed: 8756289]
4. Fuller, MT. Spermatogenesis. In: Bate, M.; Martinez Arias, A., editors. The Development of Drosophila. Cold Spring Harbor Press; Cold Spring Harbor: 1993. p. 71-147.
5. Williamson A, Lehmann R. Germ cell development in Drosophila. Annu Rev Cell Dev Biol 1996;12:365–91. [PubMed: 8970731]
6. Gönczy P, Matunis E, DiNardo S. *bag-of-marbles* and *benign gonial cell neoplasm* act in the germline to restrict proliferation during Drosophila spermatogenesis. Development 1997;124:4361–71. [PubMed: 9334284]
7. Hime GR, Brill JA, Fuller MT. Assembly of ring canals in the germ line from structural components of the contractile ring. J Cell Sci 1996;109:2779–88. [PubMed: 9013326]
8. de Cuevas M, Lilly MA, Spradling AC. Germline cyst formation in Drosophila. Annu Rev Genet 1997;31:405–28. [PubMed: 9442902]
9. Arama E, Agapite J, Steller H. Caspase activity and a specific cytochrome *c* are required for sperm differentiation in Drosophila. Dev Cell 2003;4:687–97. [PubMed: 12737804]
10. Cagan RL. Spermatogenesis: borrowing the apoptotic machinery. Curr Biol 2003;13:600–2.
11. Fabrizio JJ, Hime G, Lemmon SK, Bazinet C. Genetic dissection of sperm individualization in *Drosophila melanogaster*. Development 1998;125:1833–43. [PubMed: 9550716]
12. Noguchi T, Miller KG. A role for actin dynamics in individualization during spermatogenesis in *Drosophila melanogaster*. Development 2003;130:1805–16. [PubMed: 12642486]
13. Steller H. Regulation of apoptosis in Drosophila. Cell Death Differ 2008;15:1132–8. [PubMed: 18437164]
14. Tokuyasu KT, Peacock WJ, Hardy RW. Dynamics of spermiogenesis in *Drosophila melanogaster*. Z Zellforsch mikros Anat 1972;127:492–525.
15. Wright TRF, Hodgetts RB, Sherald AF. The genetics of dopa decarboxylase in *Drosophila melanogaster* I. Isolation and characterization of deficiencies that delete the dopa-decarboxylase-dosage-sensitive region and the α-methyl-dopa-hypersensitive locus. Genetics 1976;84:267–85. [PubMed: 826447]
16. Sharma, Y. Biological Sciences. University of Iowa; Iowa City: 2004. The Drosophila deafness gene *beethoven* encodes the Dynein Heavy Chain 1b isoform required for intraflagellar transport.
17. Caldwell JC, Fineberg SK, Eberl DF. *reduced ocelli* encodes the leucine rich repeat protein *Pray For Elves* in *Drosophila melanogaster*. Fly 2007;1:146–52. [PubMed: 18820435]

18. Tauber E, Eberl DF. Song production in auditory mutants of Drosophila: the role of sensory feedback. J Comp Physiol A 2001;187:341–8. [PubMed: 11529478]
19. Tauber E, Eberl DF. Acoustic communication in Drosophila. Behav Proc 2003;64:197–210.
20. Baker JD, Adhikarakunnathu S, Kernan MJ. Mechanosensory-defective, male-sterile *unc* mutants identify a novel basal body protein required for ciliogenesis in Drosophila. Development 2004;131:3411–22. [PubMed: 15226257]
21. Caldwell JC, Eberl DF. Towards a molecular understanding of Drosophila hearing. J Neurobiol 2002;53:172–89. [PubMed: 12382274]
22. Eberl DF, Hardy RW, Kernan M. Genetically similar transduction mechanisms for touch and hearing in Drosophila. J Neurosci 2000;20:5981–8. [PubMed: 10934246]
23. Kernan M, Cowan D, Zuker C. Genetic dissection of mechanosensory transduction: mechanoreception-defective mutations of Drosophila. Neuron 1994;12:1195–206. [PubMed: 8011334]
24. Eberl DF, Duyk GM, Perrimon N. A genetic screen for mutations that disrupt an auditory response in *Drosophila melanogaster*. Proc Natl Acad Sci (USA) 1997;94:14837–42. [PubMed: 9405700]
25. Stapleton M, Carlson J, Brokstein P, Yu C, Champe M, George R, Guarin H, Kronmiller B, Pacleb J, Park S, Wan K, Rubin GM, Celniker SE. A Drosophila full-length cDNA resource. Genome Biol 2002;3:1–8.
26. Xu D, Li Y, Arcaro M, Lackey M, Bergmann A. The CARD-carrying caspase Dronc is essential for most, but not all, developmental cell death in Drosophila. Development 2005;132:2125–34. [PubMed: 15800001]
27. Ryoo HD, Bergmann A, Gonen H, Ciechanover A, Steller H. Regulation of Drosophila IAP1 degradation and apoptosis by *reaper* and *ubcD1*. Nature Cell Biol 2002;4:432–8. [PubMed: 12021769]
28. Cadavid ALM, Ginzel A, Fischer JA. The function of the Drosophila Fat facets deubiquitinating enzyme in limiting photoreceptor cell number is intimately associated with endocytosis. Development 2000;127:1727–36. [PubMed: 10725248]
29. Barolo S, Castro B, Posakony JW. New Drosophila transgenic reporters: insulated P-element vectors expressing fast-maturing RFP. Biotechniques 2004;36:436–42. [PubMed: 15038159]
30. Parks AL, Cook KR, Belvin M, Dompe NA, Fawcett R, Huppert K, Tan LR, Winter CG, Bogart KP, Deal JE, Deal-Herr ME, Grant D, Marcinko M, Miyazaki WY, Robertson S, Shaw KJ, Tabios M, Vysotskaia V, Zhao L, Andrade RS, Edgar KA, Howie E, Killpack K, Milash B, Norton A, Thao D, Whittaker K, Winner MA, Friedman L, Margolis J, Singer MA, Kopczynski C, Curtis D, Kaufman TC, Plowman GD, Duyk G, Francis-Lang HL. Systematic generation of high-resolution deletion coverage of the *Drosophila melanogaster* genome. Nature Genet 2004;36:288–92. [PubMed: 14981519]
31. Brand AH, Perrimon N. Targeted gene expression as a means of altering cell fates and generating dominant phenotypes. Development 1993;118:401–15. [PubMed: 8223268]
32. Sharma Y, Cheung U, Larsen EW, Eberl DF. pPTGAL, a convenient Gal4 P-element vector for testing expression of enhancer fragments in Drosophila. Genesis 2002;34:115–8. [PubMed: 12324963]
33. Wilson RL, Goodman JL, Strelets VB. The Flybase Consortium. Flybase: integration and improvements to query tools. Nucl Acids Res 2008;36:588–93.
34. Saurin AJ, Borden KLB, Boddy MN, Freemont PS. Does this have a familiar RING? Trends Biochem Sci 1996;21:208–14. [PubMed: 8744354]
35. Freemont PS. Ubiquitination: RING for destruction? Curr Biol 2000;10:84–7.
36. Lorick KL, Jensen JP, Fang S, Ong AM, Hatakeyama S, Weissman AM. RING fingers mediate ubiquitin-conjugating enzyme (E2)-dependent ubiquitination. Proc Natl Acad Sci (USA) 1999;96:11364–9. [PubMed: 10500182]
37. Wilson R, Goyal L, Ditzel M, Zachariou A, Baker DA, Agapite J, Steller H, Meier P. The DIAP1 RING finger mediates ubiquitination of Dronc and is indispensible for regulating apoptosis. Nature Cell Biol 2002;4:445–50. [PubMed: 12021771]
38. Roseman RR, Johnson EA, Rodesch CK, Bjerke M, Nagoshi RN, Geyer PK. A P element containing *suppressor of Hairy-wing* binding regions has novel properties for mutagenesis in *Drosophila melanogaster*. Genetics 1995;141:1061–74. [PubMed: 8582613]

39. Thibault ST, Singer MA, Miyazaki WY, Milash B, Dompe NA, Singh CM, Buchholz R, Demsky M, Fawcett R, Francis-Lang HL, Ryner L, Cheung LM, Chong A, Erickson C, Fisher WW, Greer K, Hartouni SR, Howie E, Jakkula L, Joo D, Killpack K, Laufer A, Mazzotta J, Smith RD, Stevens LM, Stuber C, Tan LR, Ventura R, Woo A, Zakrajsek I, Zhao L, Chen F, Swimmer C, Kopczynski C, Duyk G, Winberg ML, Margolis J. A complementary transposon tool kit for *Drosophila melanogaster* using *P* and *piggyBac*. Nature Genet 2004;36:283–7. [PubMed: 14981521]
40. Kiehart DP, Galbraith CG, Edwards KL, Rickoll WL, Montague RA. Multiple forces contribute to cell sheet morphogenesis for dorsal closure in Drosophila. J Cell Biol 2000;149:471–90. [PubMed: 10769037]
41. Yao KM, White K. Neural specificity of *elav* expression: defining a Drosophila promotor for directing expression to the nervous system. J Neurochem 1994;63:41–51. [PubMed: 8207445]
42. Hayashi S, Ito K, Sado Y, Taniguchi M, Akimoto A, Takeuchi H, Aigaki T, Matsuzaki F, Nakagoshi H, Tanimura T, Ueda R, Uemura T, Yoshihara M, Goto S. GETDB, a database compiling expression patterns and molecular locations of a collection of Gal4 enhancer traps. Genesis 2002;34:58–61. [PubMed: 12324948]
43. Cherbas L, Hu X, Zhimulev I, Belyaeva E, Cherbas P. EcR isoforms in Drosophila: testing tissue-specific requirements by targeted blockade and rescue. Development 2003;130:271–84. [PubMed: 12466195]
44. Freeman M. Reiterative use of the EGF receptor triggers differentiation of all cell types in the Drosophila eye. Cell 1996;87:651–60. [PubMed: 8929534]
45. Nishito Y, Hasegawa M, Inohara N, Núñez G. MEX is a testis-specific E3 ubiquitin ligase that promotes death receptor-induced apoptosis. Biochem J 2006;396:411–7. [PubMed: 16522193]
46. Meier P, Silke J, Leevers SJ, Evan GI. The Drosophila caspase DRONC is regulated by DIAP1. EMBO J 2000;19:598–611. [PubMed: 10675329]
47. Bergmann A, Yang AY-P, Srivastava M. Regulators of IAP function: coming to grips with the grim reaper. Curr Opin Cell Biol 2003;15:717–24. [PubMed: 14644196]
48. Grether ME, Abrams JM, Agapite J, White K, Steller H. The *head involution defective* gene of *Drosophila melanogaster* functions in programmed cell death. Genes Dev 1995;9:1694–704. [PubMed: 7622034]
49. White K, Tahaoglu E, Steller H. Cell killing by the Drosophila gene *reaper*. Science 1996;9:805–7. [PubMed: 8628996]
50. Hay BA, Wassarman DA, Rubin GM. Drosophila homologs of baculovirus inhibitor of apoptosis proteins function to block cell death. Cell 1995;83:1253–62. [PubMed: 8548811]
51. Hays R, Wickline L, Cagan R. Morgue mediates apoptosis in the *Drosophila melanogaster* retina by promoting degradation of DIAP1. Nature Cell Biol 2002;4:425–31. [PubMed: 12021768]
52. Holley CL, Olson MR, Colón-Ramos DA, Kornbluth S. Reaper eliminates IAP proteins through stimulated IAP degradation and generalized translational inhibition. Nature Cell Biol 2002;4:439–44. [PubMed: 12021770]
53. Yoo SJ, Huh JR, Muro I, Yu H, Wang L, Wang SL, Feldman RMR, Clem RJ, Müller H-AJ, Hay BA. Hid, Rpr and Grim negatively regulate DIAP1 levels through distinct mechanisms. Nature Cell Biol 2002;4:416–24. [PubMed: 12021767]
54. Dorstyn L, Colussi PA, Quinn LM, Richardson H, Kumar S. DRONC, an ecdysoneinducible Drosophila caspase. Proc Natl Acad Sci (USA) 1999;96:4307–12. [PubMed: 10200258]
55. Quinn LM, Dorstyn L, Mills K, Colussi PA, Chen P, Coombe M, Abrams J, Kumar S, Richardson H. An essential role for the caspase Dronc in developmentally programmed cell death in Drosophila. J Biol Chem 2000;275:40416–24. [PubMed: 10984473]
56. Fraser AG, McCarthy NJ, Evan GI. drICE is an essential caspase required for apoptotic activity in Drosophila cells. EMBO J 1997;16:6192–9. [PubMed: 9321398]
57. Kaiser WJ, Vucic D, Miller LK. The Drosophila inhibitor of apoptosis D-IAP1 suppresses cell death induced by the caspase drICE. FEBS Lett 1998;440:243–8. [PubMed: 9862464]
58. Vucic D, Kaiser WJ, Miller LK. Inhibitor of apoptosis proteins physically interact with and block apoptosis induced by Drosophila proteins HID and GRIM. Molec Cell Biol 1998;18:3300–9. [PubMed: 9584170]

59. Wing JP, Schreader BA, Yokokura T, Wang Y, Andrews PS, Huseinovic N, Dong CK, Ogdahl JL, Schwartz LM, White K, Nambu JR. Drosophila Morgue is an F box/ubiquitin conjugase domain protein important for grim-reaper mediated apoptosis. Nature Cell Biol 2002;4:451–6. [PubMed: 12021772]

60. Rodrigues A, Oliver H, Zou H, Chen P, Wang X, Abrams JM. Dark is a Drosophila homologue of Apaf-1/CED-4 and functions in an evolutionarily conserved death pathway. Nature Cell Biol 1999;1:272–9. [PubMed: 10559939]

61. Song Z, McCall K, Steller H. DCP-1, a Drosophila cell death protease essential for development. Science 1997;275:536–40. [PubMed: 8999799]

62. Geisbrecht ER, Montell DJ. A role for Drosophila IAP1-mediated caspase inhibition in Rac-dependent cell migration. Cell 2004;118:111–25. [PubMed: 15242648]

63. Zhao M, Szafranski P, Hall CA, Goode S. Basolateral junctions utilize Warts signaling to control epithelial-mesenchyme transition and proliferation crucial for migration and invasion of Drosophila ovarian epithelial cells. Genetics 2008;178:1947–71. [PubMed: 18430928]

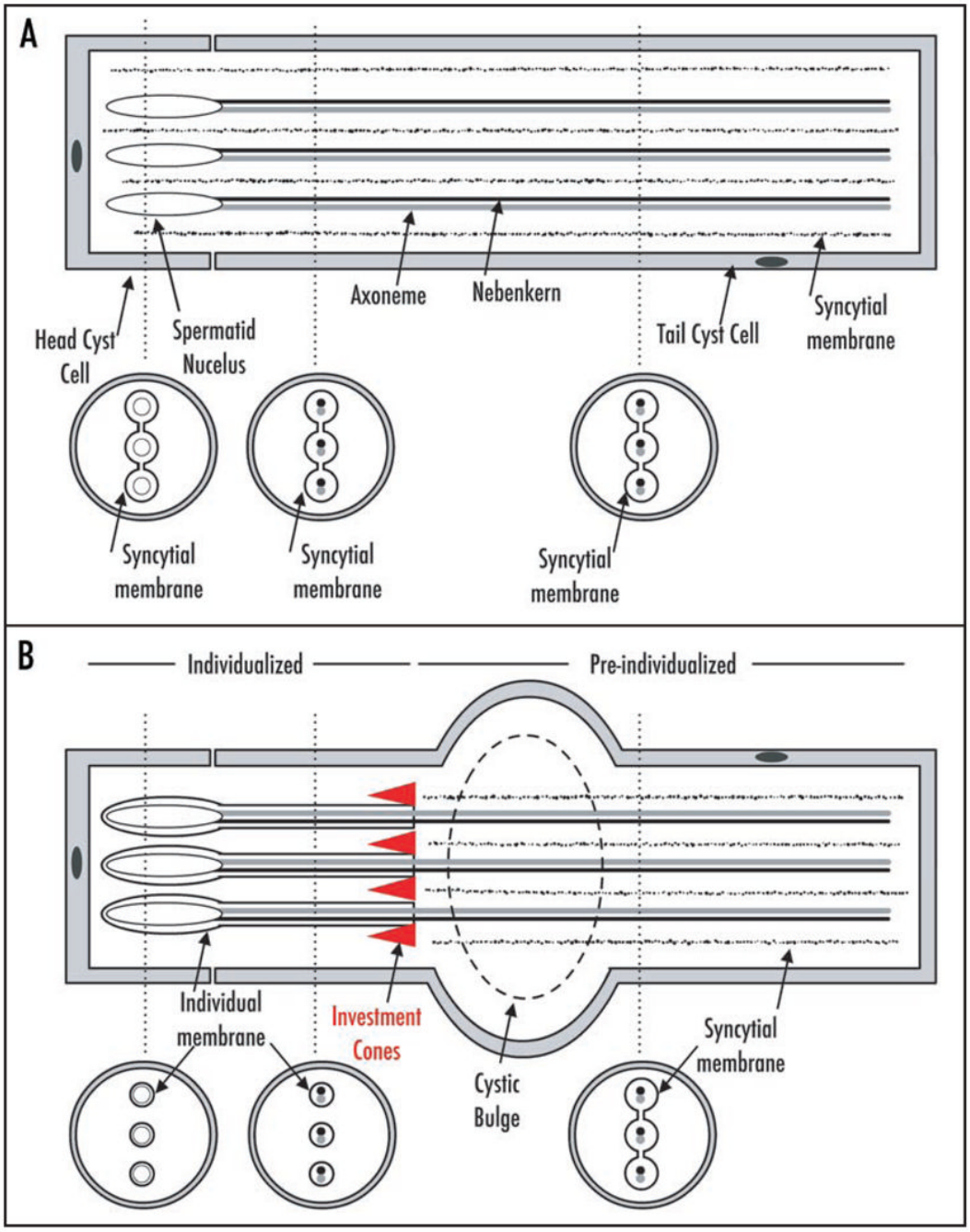

Figure 1.

Spermatid individualization. (A) Following elongation of the axoneme, mitochondria and the tail cyst cell, the head cyst cell-associated spermatid nuclei condense into needle-like morphologies. For clarity, only three of the 64 spermatid units are shown. The spermatids are still connected by a syncytial membrane (jagged lines). The vertical dashed lines indicate areas diagrammed in cross-section below. The interconnected syncyctial membrane surrounding the various spermatid structures is shown (thick black incomplete circles). (B) The investment cones (triangles) travel the length of the spermatids to (1) individualize each member of the 64-unit bundle in its own plasma membrane and (2) remove the shared, syncytial cytoplasm. These cones have already individualized the spermatid nuclei and some of the axoneme/

nebenkern. As the investment cones travel caudally (rightward), the cytoplasmic waste is collected and forms a so-called cystic bulge. At the end of individualization the waste bag is removed (not shown). In (B), the individualized areas are indicated by thick black circles representing membranes tightly surrounding the spermatid structures while the pre-individualized areas are indicated by thick black incomplete circles.

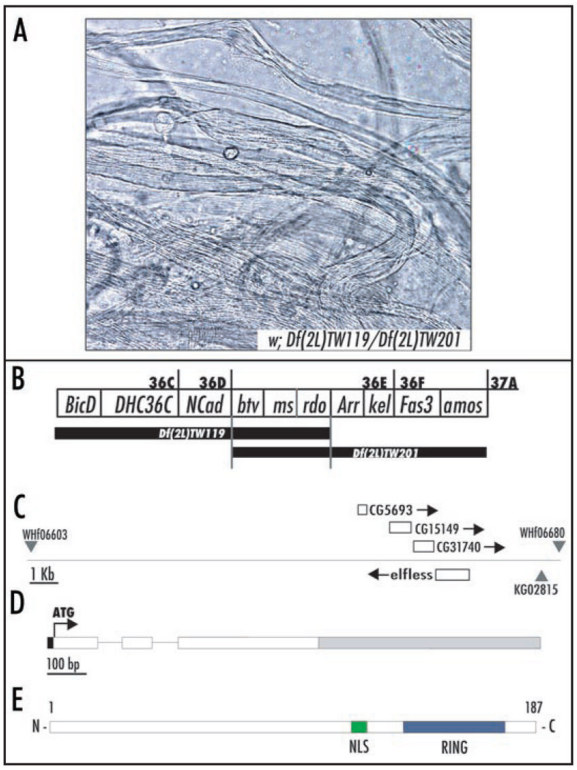

Figure 2.

The *btv*-male sterile-*rdo* overlapping deficiency region. (A) Representative squash of *Df/Df* testes showing amotile sperm that remain encysted. (B) The genetic map of the *btv*-male sterile-*rdo* region derived from overlapping deficiencies *TW119* and *TW201*. In the flanking regions uncovered by only one of the deficiencies, only some loci are listed. (C) A subregion of the larger *Df/Df* including *elfless* and three other small predicted genes (*btv* and CG5674 are not shown at this magnification). Arrows indicate the direction of transcription. Positions of transposable element insertions used in this study are shown by grey triangles. (D) The *elfless* intronexon structure shows the three exons (boxes) connected by two introns (thin lines). The 5′UTR (black box) and 3′UTR (grey box) are also indicated. (E) The predicted domain structure of the *elfless* protein contains a nuclear localization signal (NLS; green box) and C-terminal RING domain (blue box).

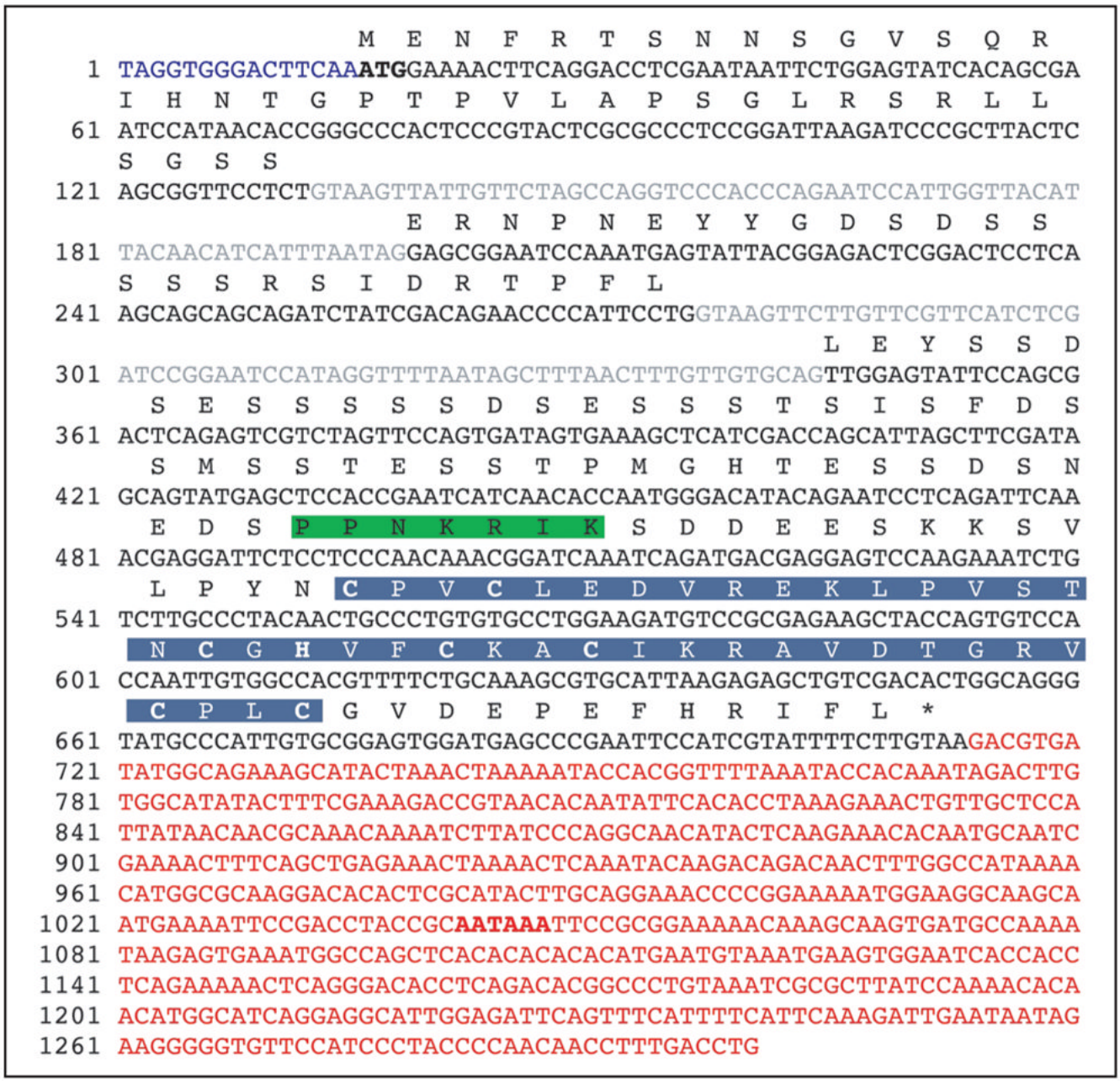

Figure 3.

The *elfless* nucleotide and amino acid sequences. The *elfless* 5′UTR is shown in blue, exons are in black (ATG start codon in bold), introns in grey and the 3′UTR in red with putative polyadenylation site (AATAAA) in bold. The *elfless* protein consists of a C3HC4-type RING domain (blue shaded box region with consensus Cys and His residues indicated in bold) and a nuclear localization signal (green box). These sequences are based on the AT24563 cDNA clone structure.

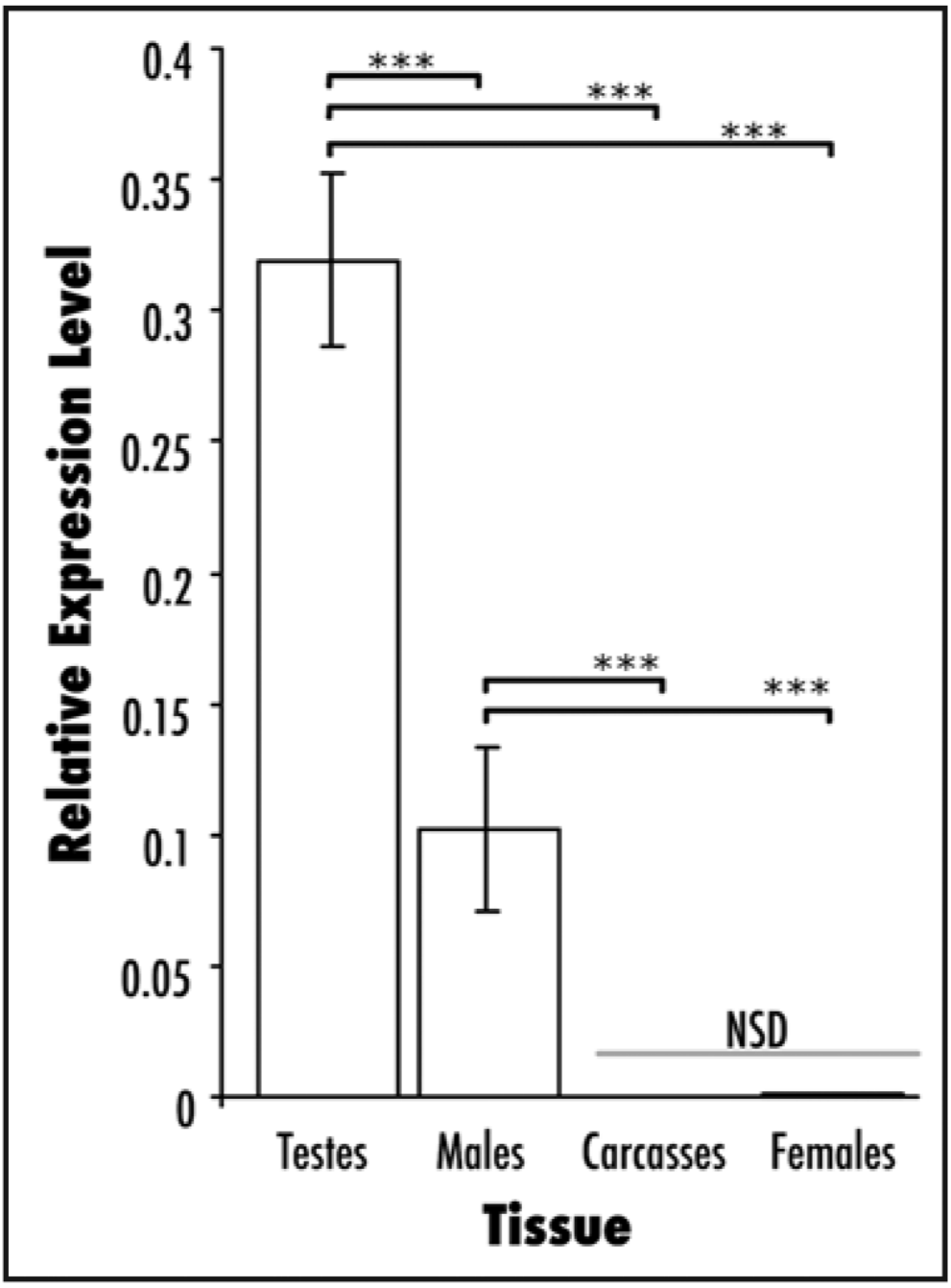

Figure 4.

elfless transcripts are greatly enhanced in testes. Levels of *elfless* transcripts, isolated from various tissues, relative to *Gapdh2* control transcripts. *elfless* is most abundant in testes (~1 copy of *elfless* for every 3 copies of *Gapdh2*), and is less abundant in whole males. *elfless* is nearly undetectable in carcasses (males with testes removed) and females. *elfless* expression in testes is significantly greater than all other tissues ($p < 0.001$ ANOVA/Tukey) and likewise *elfless* transcript levels in whole males is greater than carcasses and females (***$p < 0.001$ ANOVA/Tukey). *elfless* expression levels do not distinguishably differ between carcasses and females.

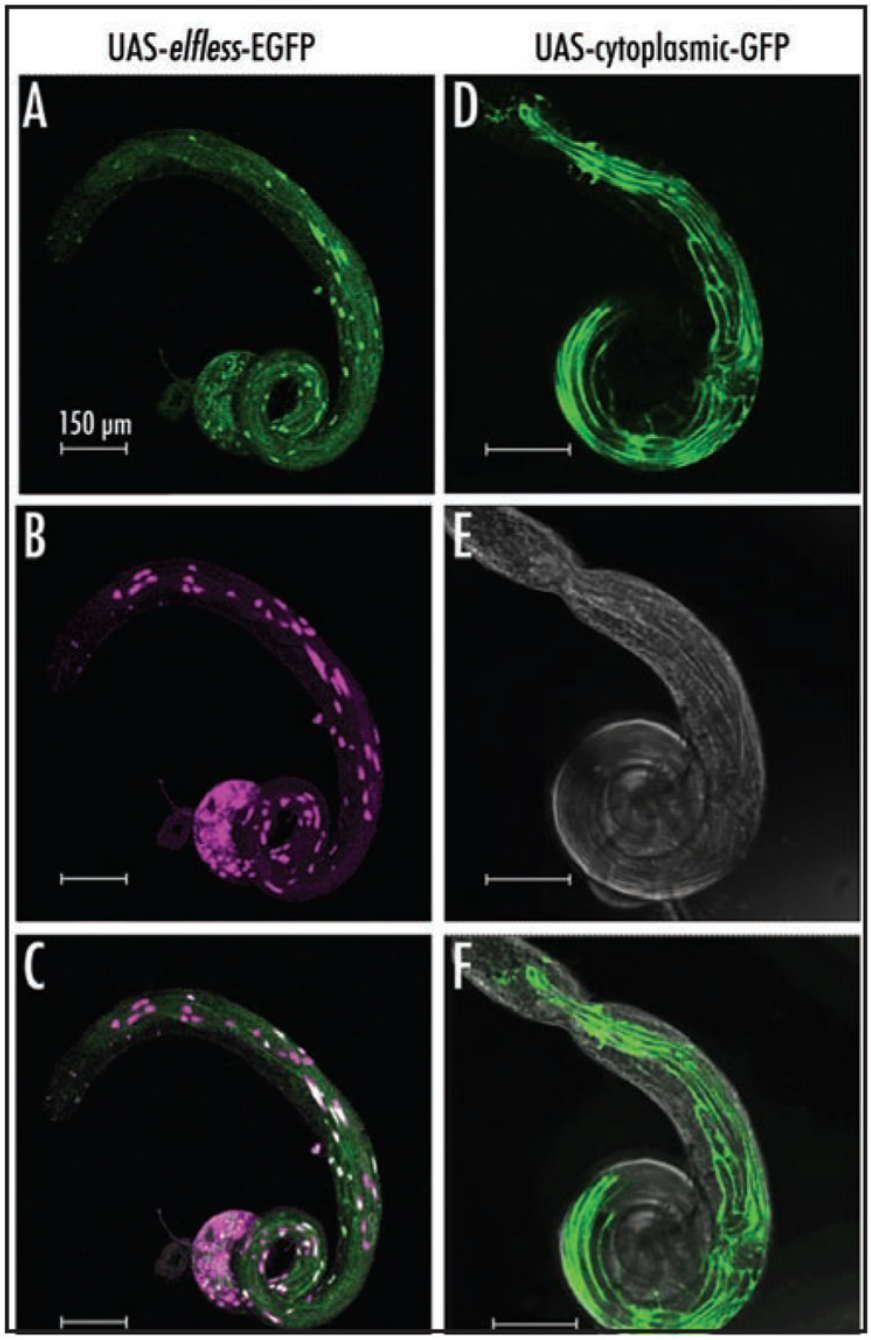

Figure 5.

elfless is expressed in testes. All UAS-constructs are driven by *elfless*-Gal4 and the expression pattern is restricted to the testes. ((A–C), UAS-*elfless*-EGFP; (D–F) UAS-cytoplasmic-GFP) (A) UAS-*elfless*-EGFP expression is limited to the tail cyst cell nuclei, confirming the predicted nuclear localization signal for *elfless.* (B) nuc*Ds*Red co-localizes with *elfless*-EGFP in the tail cyst cell nuclei and also exhibits significant spurious expression (independent of Gal4 driver) in the spermatid and head cyst cell nuclei (non co-localized regions in C). (C) Merge of (A and B). (D) UAS-cytoplasmic-GFP expression (without nuclear localization signal) is seen throughout the tail cyst cell. (E) DIC (F) Merge of (D and E). Scale bars = 150 μm.

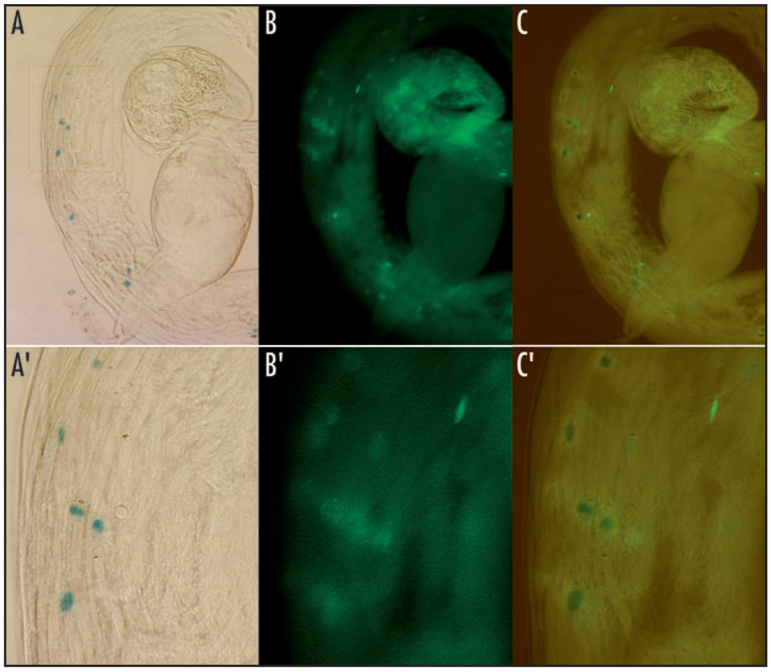

Figure 6.
Elfless-EGFP is co-expressed with a tail cyst cell marker. A testis from a male with *elfless*-Gal4 driving UAS-*elfless*-EGFP in the presence of the tail cyst cell enhancer trap *P{lacW} 498* was processed for X-gal staining to reveal the tail cyst cell nuclei (A and A′). Sufficient EGFP fluorescence remained in these testes for imaging despite some increased background (B and B′). Imaging both simultaneously (C and C′) shows significant co-incidence of Elfless-EGFP and enhancer trap expression. The red box in (A) indicates the region shown at higher magnification in (A′–C′).

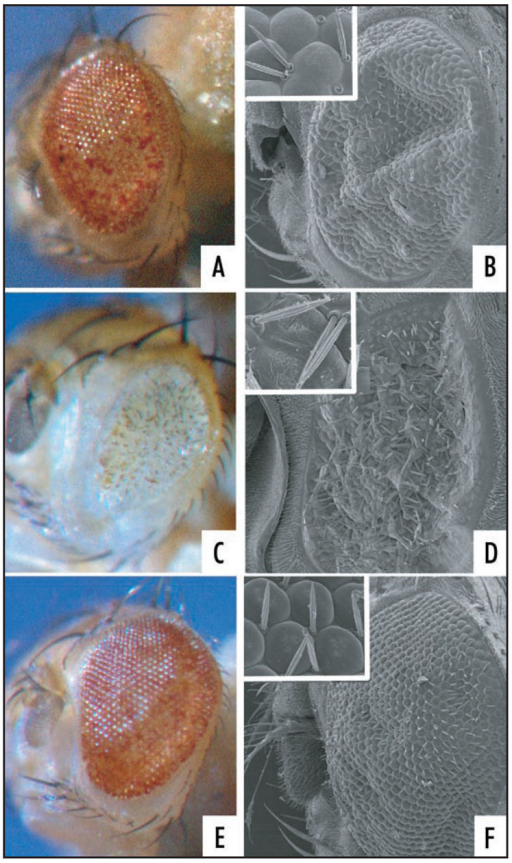

Figure 7.

Ectopic mis-expression of *elfless* induces apoptosis. (A, C and E) Light microscopy (B, D and F) SEM with insets. (A and B) *w*; *GMR*-Gal4/+; UAS-*elfless/+* flies exhibit pigment loss and other defects such as loss or duplication of the interommatidial bristles and often the eye surface morphology is irregular. (C and D) *w*; *GMR*-Gal4/+; UAS-*elfless/ubcD1* flies exhibit almost complete pigment loss and severe bristle and eye shape/size phenotypes and this genetic combination shows reduced viability. (E and F) *w*; *GMR*-Gal4/+; UAS-*elfless/Dronc* flies exhibit less severe pigment and morphological defects than *w*; *GMR*-Gal4/+; UAS-*elfless/+* alone.

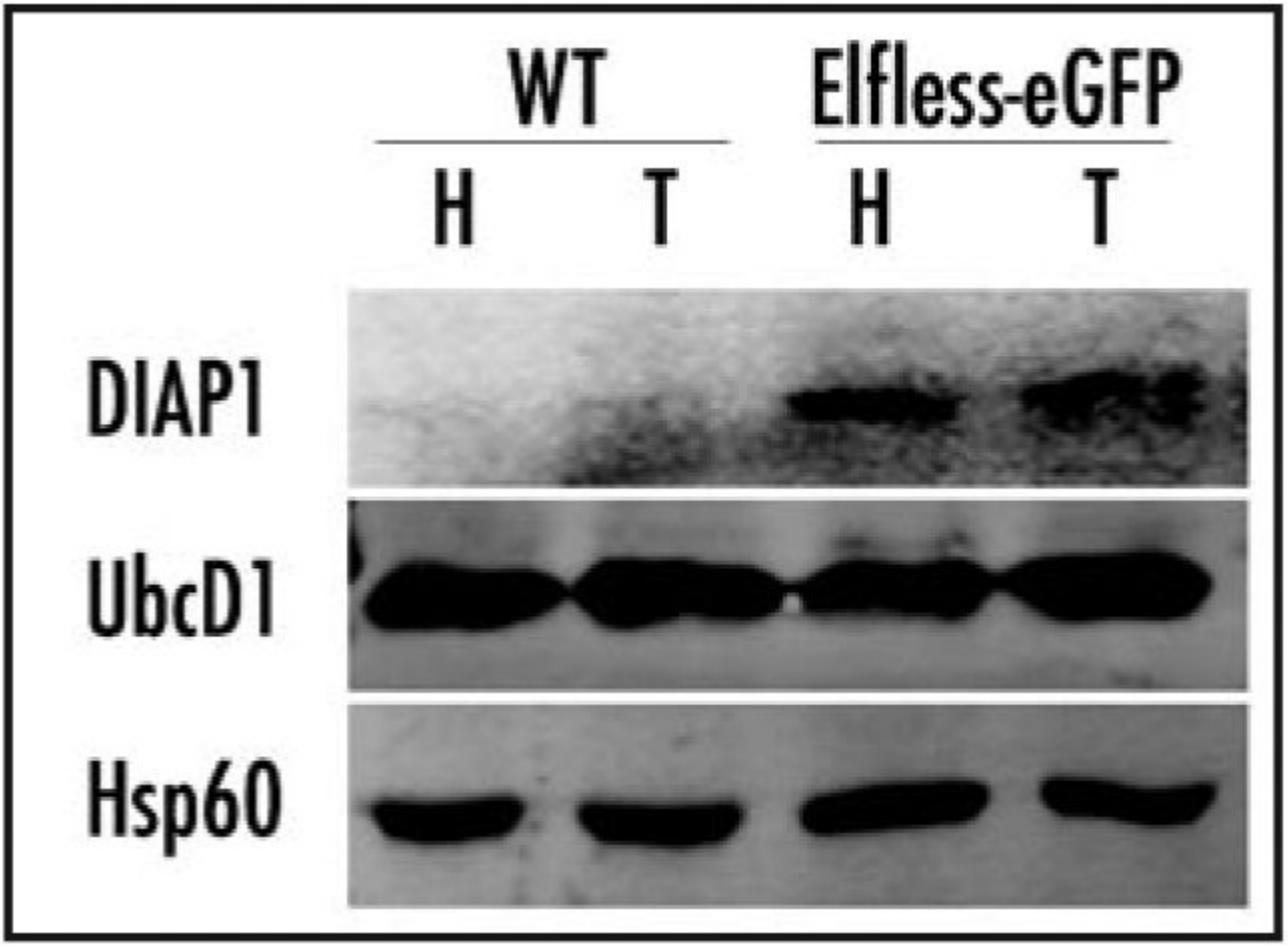

Figure 8.

DIAP1, but not UbcD1, is increased upon Elfless expression. Western blot of protein isolated from GMR-Gal4 control heads (H), or Elfless-Gal4 control testes (T), was probed with antibodies against DIAP1, UbcD1 or the loading control, Hsp60. Compared to these controls (labeled WT), protein extracts of the corresponding tissues from their siblings, which also carry the UAS-elfless-EGFP construct (labeled Elfless-eGFP), show increased levels of DIAP1, but no change in UbcD1 levels is evident.

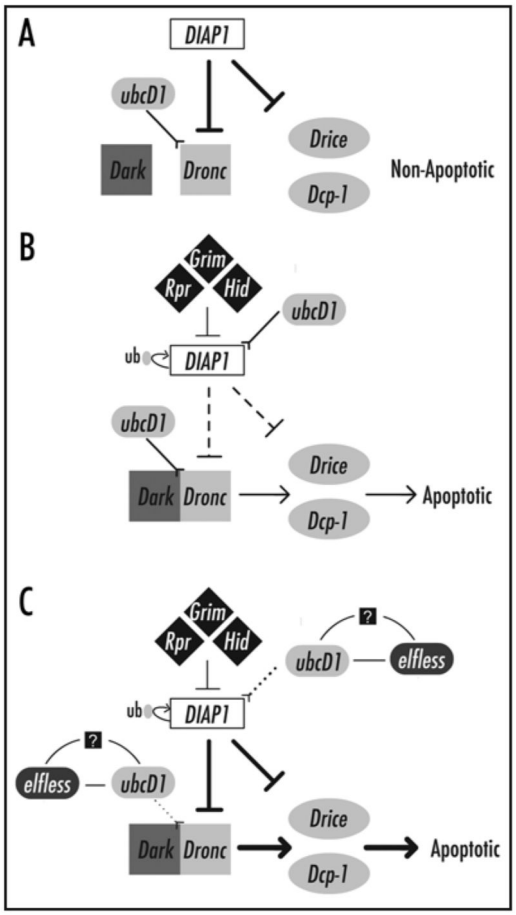

Figure 9.

Model for *elfless* in apoptosis. In these simplified models of apoptosis, the strength of inhibition (t-bars), activation (arrowheads) or ubiquitination (inverted arrowheads) is represented by line weight. (A) In a wild type non-apoptotic cell, the key regulatory molecule is *DIAP1*. This protein inhibits the downstream activator caspase, *Dronc*, and the effector caspases *(Drice* and *Dcp-1*). Likewise, *Dronc* is a target of *ubcD1*-dependent ubiquitination. (B) When a wild type cell receives an intrinsic or extrinsic signal to die, the pro-apoptotic genes, *Grim-Rpr-Hid* inhibit *DIAP1* and *DIAP1* auto-ubiquitinates in a *ubcD1*-dependent manner. The downstream caspases are no longer strongly inhibited and the cell becomes apoptotic. In this genetic background, two copies of *ubcD1* are present and therefore a significant level of ubiquitination of *Dronc* is evident and this balance prevents "excessive" cell death. (C) In this model for the role *elfless* as a direct or indirect (black box) negative regulator of *ubcD1* activity. When *elfless* is mis-expressed with *GMR*-Gal4 *ubcD1* is strongly inhibited. This presumably results in strong suppression of caspsases by *DIAP1*, but since *ubcD1* also acts further downstream, the increased apoptosis is attributable to mis-regulation of *Dronc* by downregulation of *ubcD1* by *elfless*. Consistent with this model, this effect is exacerbated in *ubcD1* heterozygotes and is attenuated in *Dronc* heterozygotes.

Table 1

Primers used in this study

Primer name	Primer sequence
elfless-FullF	5′-CACAGCGAATCCATAACACCG-3′
elfless-FullR	5′-GGTCAAAGGTTGTTGGGGTAG-3′
CG31740Fwd	5′-GTGGGATTCGAAACCTAGAG-3′
CG31740Rev	5′-CTATGATAGCGGGCGCTTCAC-3′
CG15149Fwd	5′-GTCCTCGTCTGTGGATCAC-3′
CG15149Rev	5′-CTCCTCTTCGGTTAATTCTG-3′
CG5693Fwd	5′-GCACCCAGTTAGCATCTATG-3′
CG5693Rev	5′-GGTTGTGTGTTCAGCACATCTC-3′
elf-GWF	5′-CACCATGGAAAACTTCAGGACC-3′
elf-GWRv2	5′-CAAGAAATTACGATGGAAATTCGGGGC-3′
SKF-5′F	5′-GGCATTAATACGGCAGCAAG-3′
SKF-5′R	5′-CACACGAGTAGTTACCTCTG-3′
Gapdh2-f	5′-AGCGCTGGTGCCGAATAC-3′
Gapdh2-r	5′-AGTGAGTGGATGCCTTGTCGAT-3′
elfless-realtimeF	5′-TGTCCGCGAGAAGCTACCA-3′
elfless-realtimeR	5′-GCACGCTTTGCAGAAAACG-3′